European Radiology (2019) 29:161–167
https://doi.org/10.1007/s00330-018-5598-5

COMPUTED TOMOGRAPHY

Neointimal formation after carotid artery stenting: phantom and clinical evaluation of model-based iterative reconstruction (MBIR)

Kazushi Yokomachi[1,2] · Fuminari Tatsugami[2] · Toru Higaki[2] · Shinji Kume[1] · Shigeyuki Sakamoto[3] · Takahito Okazaki[3] · Kaoru Kurisu[3] · Yuko Nakamura[2] · Yasutaka Baba[2] · Makoto Iida[2] · Kazuo Awai[2]

Received: 12 April 2018 / Revised: 30 May 2018 / Accepted: 6 June 2018 / Published online: 22 June 2018

Abstract

Objectives The objective of this study was to investigate the usefulness of model-based iterative reconstruction (IR) for detecting neointimal formations after carotid artery stenting.

Methods In a cervical phantom harbouring carotid artery stents, we placed simulated neointimal formations measuring 0.40, 0.60, 0.80 and 1.00 mm along the stent wall. The thickness of in-stent neointimal formations was measured on images reconstructed with filtered-back projection (FBP), hybrid IR (AIDR 3D), and model-based IR (FIRST). The clinical study included 43 patients with carotid stents. Cervical computed tomography (CT) images obtained on a 320-slice scanner were reconstructed with AIDR 3D and FIRST. Five blinded observers visually graded the likelihood of neointimal formations on AIDR 3D and AIDR 3D plus FIRST images. Carotid ultrasound images were the reference standard. We analysed results of visual grading by using a Jack-knife type receiver observer characteristics analysis software.

Results In the phantom study, the difference between the measured and the true diameter of the neointimal formations was smaller on FIRST than FBP or AIDR 3D images. In the clinical study, the sensitivity, specificity, positive predictive value, negative predictive value and accuracy of AIDR 3D were 58%, 88%, 83%, 67% and 73%, respectively. For AIDR 3D plus FIRST images they were 84%, 78%, 80%, 82% and 81%, respectively. The mean area under the curve was significantly higher on AIDR 3D plus FIRST than AIDR 3D images (0.82 vs 0.72; $p < 0.01$).

Conclusions The model-based IR algorithm helped to improve diagnostic performance for the detection of neointimal formations after carotid artery stenting.

Key Points

- *Neointimal formations can be visualised more accurately with model-based IR.*
- *Model-based IR improves the detection of neointimal formations after carotid artery stenting.*
- *Model-based IR is suitable for follow up after carotid artery stenting.*

Keywords CT angiography · Carotid artery stenosis · Image reconstruction · Multidetector computed tomography · Image quality enhancement

✉ Kazushi Yokomachi
yokomach@hiroshima-u.ac.jp

[1] Department of Radiology, Hiroshima University Hospital, Kasumi 1-2-3, Minami-ku, Hiroshima 734-8551, Japan

[2] Department of Diagnostic Radiology, Graduate School of Biomedical and Health Sciences, Hiroshima University, Kasumi 1-2-3, Minami-ku, Hiroshima 734-8551, Japan

[3] Department of Neurosurgery, Hiroshima University Hospital, Kasumi 1-2-3, Minami-ku, Hiroshima 734-8551, Japan

Abbreviations

AIDR 3D	Three-dimensional adaptive iterative dose reduction
CAS	Carotid artery stenting
FBP	Filtered-back projection
FIRST	Forward-projected model-based iterative reconstruction solution
IR	Iterative reconstruction

Introduction

Carotid endarterectomy is used to remove the vascular intima; it is the standard treatment for carotid stenosis [1, 2]. However, it is highly invasive and performed under general anaesthesia. Carotid artery stenting (CAS) is less invasive than surgery and can be performed endovascularly. Due to technical advances and improved stent-related materials [3], it is now performed widely in recent years. However, within 2 years of undergoing CAS, 4-8% of patients present with restenosis [4, 5].

Ultrasound study is primarily used to evaluate the development of neointimal formations for patients who have undergone CAS [4–6]. They are non-invasive and of higher spatial resolution than computed tomography (CT) images. However, the recorded measurements can vary depending on the individual performing the procedure, and ultrasound waves are attenuated in distal regions of the carotid artery [7, 8].

On CT images, the entire carotid artery can be evaluated uniformly, and findings are not reader-dependent. However, when CT angiography obtained with filtered-back projection (FBP) or hybrid iterative reconstruction (IR) is used for post-stenting evaluation, blooming artefacts render stent struts thicker than they actually are because stents are made of materials that absorb high levels of radiation [9]. Consequently, neointimal formations can be overlooked.

Model-based IR is an image reconstruction technique that accurately reproduces CT values without FBP. Its spatial resolution is higher than on images reconstructed with conventional FBP or hybrid IR and its sophisticated modelling is expected to reduce blooming artefacts and improve the image quality compared to hybrid IR [10–12]. Model-based IR may facilitate the detection of subtle or fine neointimal formations developed inside stents after CAS.

To the best of our knowledge, the usefulness of model-based IR for detecting neointimal formations after carotid artery stenting has not been evaluated. The objective of this study was to evaluate and compare the diagnostic accuracy for the detection of neointimal formations after CAS on images reconstructed with hybrid and model-based IR.

Materials and methods

Phantom study

Phantom design

The phantom simulating the carotid artery was created with a three-dimensional (3D) printer (Agilista; Keyence, Breda, Belgium) (Fig. 1). It was made of ultraviolet curing acrylic resin [CT value approximately 50 Hounsfield units (HU, 120 kVp)]. The vertebrae were made of plaster (CT value approximately 1,000 HU). Two types of stents were inserted into the carotid artery, a carotid WALLSTENT (8 × 21 mm, cobalt/nichrome alloy; Boston Scientific, Malborough, MA, USA) or a PRECISE stent (8 × 20 mm, nickel/titanium alloy; Johnson & Johnson, Cordis, Bridgewater, NJ, USA). We made simulated neointimal formations with the 3D printer; their thickness was set at 0.40, 0.60, 0.80 or 1.00 mm (CT value approximately 50 HU) and they were placed in the stent. The vessel lumen was filled with diluted contrast agent (iomeprol, Iomeron 300 mgI/mL; Eisai, Tokyo, Japan) adjusted to 450 HU.

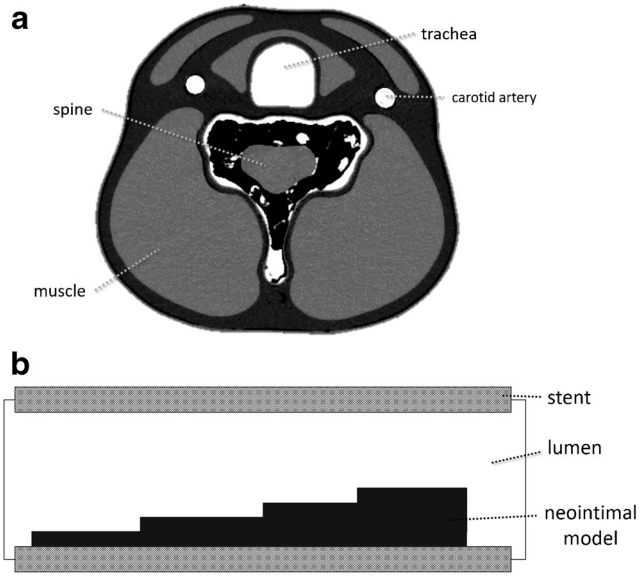

Fig. 1 Cervical phantom (**a**) harbouring a simulated carotid artery (**b**). Simulated neointimal formations (thickness 0.4, 0.6, 0.8 or 1.0 mm) were placed along the stent wall of a carotid WALLSTENT or a PRECISE stent. The vessel lumen was filled with diluted contrast medium (450 HU at 120 kVp)

Scan parameters and image analysis

Five CT scans were obtained under the same imaging conditions on a 320-slice CT scanner (Aquilion ONE; Canon Medical Systems, Otawara-shi, Japan). The scan parameters were tube voltage, 120 kVp; tube current, 300 mA; tube rotation speed, 0.4 s/rot; beam pitch, 0.844. A short-axis image was generated from images reconstructed with FBP, AIDR 3D and model-based IR (forward-projected model-based iterative reconstruction solution: FIRST) (Fig. 2). All images were reconstructed with FBP using a sharp kernel (FC15), AIDR 3D (standard setting) using a sharp kernel (FC15), and with FIRST (cardiac setting). The thickness of neointimal formations (0.40, 0.60, 0.80 and 1.00 mm) was measured using a profile curve on short-axis images obtained with each reconstruction method (Fig. 3).

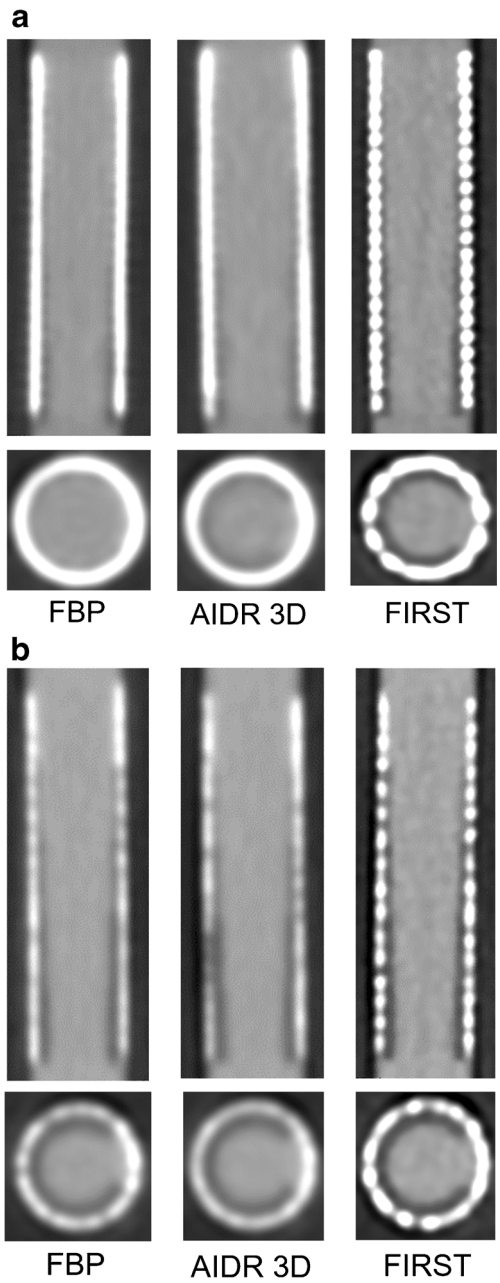

Fig. 2 Comparison of long- and short-axis images of the simulated carotid artery. The images were acquired with FBP, AIDR 3D and FIRST. **a** Carotid WALLSTENT, **b** PRECISE stent. *FBP* filtered back projection, *AIDR 3D* three-dimensional adaptive iterative dose reconstruction, *FIRST* forward projected model-based iterative reconstruction solution

Clinical study

Patient population

Our study was performed in compliance with the principles of the Declaration of Helsinki and approved by our institutional review board. Informed prior consent was obtained from all patients. Included were 43 patients (37 men, 6 women; average age, 70 years; age range, 61-83 years) who had undergone ultrasound studies within 1 month before and after CT angiography performed between March 2015 and February 2017.

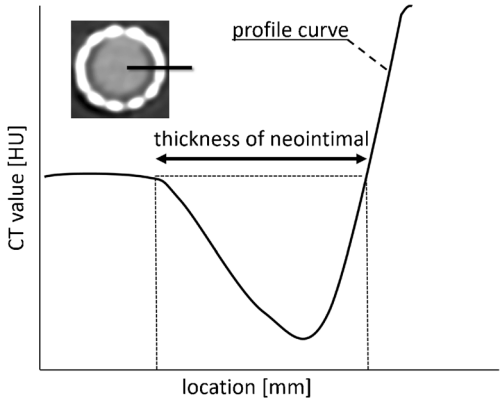

Fig. 3 Measurement of the neointimal thickness. A profile curve of the neointimal formation on a short-axis image was used. The thickness of the neointimal formation was defined as the area where the CT number was lower than that of the simulated carotid artery lumen

CT scanning and image analysis

All CT scans were performed on a 320-detector CT scanner. Using a dual-shot injector (DUAL SHOT GX7; Nemoto Kyorindo, Bunkyo-ku, Japan), we delivered 300 mgI/kg of non-ionic contrast material (iomeprol, Iomeron 300 mgI/mL; Eisai) at a fixed duration of 15 s to all patients. This was followed by 30 ml of a 0.9% saline solution injected at the same flow rate as the contrast material. The scan start time was determined using the bolus tracking method. Images were reconstructed at a slice thickness of 0.5 mm. The scan parameters were 32 × 0.5 mm; rotation time, 0.4 s; tube voltage, 120 kVp; auto exposure control index, 6; matrix, 512 × 512. All images were reconstructed with AIDR 3D (standard setting) using a sharp kernel (FC15) and with FIRST (cardiac setting). The mean thickness of the neointimal formation was measured at the narrowest point on each image reconstructed with AIDR 3D, and with FIRST. Display was on a ziostation2 workstation (Ziosoft, Tokyo, Japan).

Carotid ultrasound studies

A technologist with 22 years of experience performed the procedure and recorded the digital images. He used a LOGIQ 7 system (GE Yokogawa Medical Systems, Hino, Japan) with a 3– to 10-MHz broadband linear array transducer. In-stent neointimal formations were evaluated by high-resolution B-mode ultrasonography. Neointimal thickness was measured on short-axis images. In the clinical study, the measured thickness of neointimal formations in ultrasound examinations was defined as the reference data.

Observer performance

We used receiver operating characteristic (ROC) analysis to evaluate the diagnostic performance of radiologists for detecting instent neointimal formations. They were five board-certified radiologists with 7-31 years of experience (mean, 18.8 years). They were allowed to change the window level and width on the workstation; reading time was not limited. All recorded their confidence level on a continuous rating scale by placing marks on a line on the recording form. The left and right end of the line indicated complete confidence in the absence or presence of instent neointimal formation, respectively. Intermediate levels of confidence were indicated by the position of the mark between the two lines' termini. The distance between the left end of the line and the mark was measured and converted into an ordinal confidence rating ranging from 0-100. Each reader underwent training that involved the reading of images of two cases not included in the actual observer performance study. AIDR 3D images were evaluated first, followed by the evaluation of AIDR 3D plus FIRST images presented in a side-by-side manner.

Statistical analyses

We calculated sensitivity, specificity, positive predictive value (PPV), negative predictive value (NPV) and accuracy in detection of neointimal formation for AIDR 3D images and AIDR 3D plus FIRST images.

To compare diagnostic ability of AIDR 3D images and AIDR 3D plus FIRST images, we analysed the data by the Jack-knife type receiver observer characteristics analysis software [13]. For this analysis, we used a free statistical software provided by Chakraborty and Yoon (JAFROC 4.2.1; http://www.devchakraborty.com/). Differences of p less than 0.05 were considered statistically significant.

We evaluated interobserver agreement for identification of neointimal formation between observers. As the observers rated the confidence score for ROC study by using a continuous rating scale of range 0-100, we transformed the score to four grade scores (Grade1, 0-25; Grade 2, 26-50; Grade 3, 51-75; Grade 4, 76-100). Then, we calculated Cohen's kappa coefficients between two observers in reading AIDR 3D and AIDR 3D plus FIRST images. We calculated kappa coefficients using a commercially available statistical software (Medcalc version 11.3.7.0; MedCalc Software, Ostend, Belgium).

Results

Phantom study

In the carotid WALLSTENT, the measured values of neointimal formations of 1.00 and 0.80 mm were more accurate on FIRST than FBP and AIDR 3D images (Table 1). On FBP and AIDR 3D images neointimal formations of 0.60 and 0.40 mm were not detectable, but they were identifiable on FIRST images (measured values of 0.54 ± 0.09 and 0.40 ± 0.11 mm, respectively).

In PRECISE stents, the measured values of neointimal formations of 1.00, 0.80 and 0.60 mm were more accurate on FIRST than on FBP and AIDR 3D images (Table 2). Neointimal formation of 0.40 mm was not detected on FBP and AIDR 3D images; with FIRST, it was identifiable (measured value of 0.30 ± 0.10 mm).

Clinical study

Of our 43 patients, 4 were implanted with a PRECISE stent and 39 with a WALLSTENT. The mean interval between stent placement and CT was 9.4 ± 10.1 months (range, 1-36 months). Neointimal formation was confirmed in 19 patients (44.2%) by ultrasound examination; 2 patients harbouring a PRECISE stent and 17 with a WALLSTENT. Measured values of neointimal formations were more accurate on FIRST than AIDR 3D images (Table 3); the mean rate of differences (%) between measured values in ultrasound examinations and those on AIDR 3D or FIRST images were 25.6 ± 12.3 % (median, 18.9 %; range, 13.8-52.9 %) and 6.3 ± 6.4 % (median, 4.1 %; range, 0-20.8 %), respectively. The sensitivity, specificity, PPV, NPV and accuracy for AIDR 3D were 58%, 88%, 83%, 67% and 73%, respectively. For AIDR 3D plus FIRST they were 84%, 78%, 80%, 82% and 81%, respectively.

The area under the best-fit receiver operating characteristic curve (AUC) in identification of neointimal formation was significantly higher for AIDR 3D plus FIRST than AIDR 3D only images (0.82 vs 0.70, $p < 0.01$) (Table 4, Fig. 4). A representative case is shown in Fig. 5.

Kappa coefficients between readers were shown in Table 5. Kappa coefficients ware ranged from 0.44 to 0.91 in reading

Table 1 Measured thickness (mm) of simulated neointimal formations along the wall of the carotid WALLSTENT

Formation thickness	Reconstruction method		
	FBP	AIDR 3D	FIRST
1.0	0.80 ± 0.18	0.75 ± 0.19	0.89 ± 0.16
0.8	0.11 ± 0.16	0.53 ± 0.14	0.64 ± 0.09
0.6	Not detected	Not detected	0.54 ± 0.09
0.4	Not detected	Not detected	0.40 ± 0.11

FBP filtered back projection, *AIDR 3D* three-dimensional adaptive iterative dose reconstruction, *FIRST* forward projected model-based iterative reconstruction solution

Numbers after plus/minus indicate standard deviation

Table 2 Measured thickness (mm) of simulated neointimal formations along the wall of the PRECISE stent

Formation thickness	Reconstruction method		
	FBP	AIDR 3D	FIRST
1.0	0.94 ± 0.13	0.90 ± 0.19	0.94 ± 0.13
0.8	0.84 ± 0.12	0.77 ± 0.13	0.82 ± 0.08
0.6	0.40 ± 0.10	0.32 ± 0.18	0.55 ± 0.08
0.4	not detected	not detected	0.30 ± 0.10

FBP filtered back projection, *AIDR 3D* three-dimensional adaptive iterative dose reconstruction, *FIRST* forward projected model-based iterative reconstruction solution

Numbers after plus/minus indicate standard deviation

AIDR 3D images and 0.56 to 0.83 in reading AIDR 3D plus FIRST images.

Discussion

Ours is the first study to evaluate the diagnostic performance of carotid artery stent scans reconstructed with the model-based IR algorithm for the detection of neointimal formations. We found that it reduced blooming effects arising from the stent and improved the diagnostic performance for the detection of neointimal formations.

Although CAS is useful for the treatment of carotid artery stenosis, the risk for restenosis demands careful follow-up. Post-CAS, ultrasound studies are performed to detect in-stent neointimal formations [6, 14–16]. However, ultrasound findings can vary depending on the individual performing the procedure. Also, evaluation of the distal region of the carotid artery is sometimes difficult because of the attenuation of ultrasound waves. On CT images, on the other hand, the entire carotid artery can be evaluated uniformly and objectively, and findings are not reader-dependent.

IR algorithms can be classified into hybrid- and model-based IR. The former applies noise reduction techniques in sinogram and image spaces. The image noise is lower and streak artefacts are fewer with hybrid IR than conventional FBP [17, 18]. Model-based IR repeats both back and forward projections in the image-reconstruction process [10, 11] and the spatial

Table 3 Measured thickness of neointimal formations in 19 patients

Case	Age	Sex	Side	Stent	Thickness (mm)		
					Ultrasound	AIDR 3D	FIRST
1	73	M	L	WS	1.05	ND	0.89 (15.3)
2	68	M	L	WS	1.25	0.81 (34.8)	1.21 (2.98)
3	71	M	R	WS	0.40	ND	0.37 (6.94)
4	73	M	L	WS	1.05	0.63 (40.5)	0.89 (15.1)
5	78	M	R	PS	0.40	ND	0.32 (20.8)
6	74	M	R	WS	0.90	1.07 (18.9)	0.83 (8.13)
7	73	M	L	WS	2.55	2.10 (17.8)	2.43 (4.84)
8	67	M	L	WS	0.50	0.43 (13.9)	0.52 (4.07)
9	73	M	L	WS	3.65	2.39 (34.6)	3.71 (1.52)
10	65	M	R	WS	0.65	ND	0.63 (3.69)
11	80	M	L	PS	28.0	32.0 (14.2)	30.0 (7.14)
12	66	M	R	WS	1.80	1.52 (15.6)	1.78 (1.11)
13	83	M	R	WS	0.60	ND	0.60 (0.00)
14	65	M	L	WS	1.10	0.70 (36.4)	1.10 (0.00)
15	74	M	L	WS	2.65	1.90 (28.3)	2.60 (1.89)
16	66	M	R	WS	0.80	0.69 (13.8)	0.79 (1.25)
17	65	M	R	WS	0.95	0.70 (26.3)	0.90 (5.26)
18	65	M	L	WS	1.70	0.80 (52.9)	1.40 (17.7)
19	66	M	R	WS	1.80	1.52 (15.6)	1.78 (1.11)

WS WALLSTENT, *PS* PRECISE stent, *ND* not detected, *AIDR 3D* three-dimensional adaptive iterative dose reconstruction, *FIRST* forward projected model-based iterative reconstruction solution

Data in parentheses are the rate of differences (%) between measured values in ultrasound examinations and those on AIDR 3D or FIRST images

Table 4 AUC values in identification of neointimal formation for AIDR 3D and AIDR 3D plus FIRST images (numbers in parentheses indicate lower and upper limits of 95% confidence interval)

	AUC value	
	AIDR 3D images	AIDR 3D plus FIRST images
Reader 1	0.711	0.852
Reader 2	0.643	0.823
Reader 3	0.688	0.818
Reader 4	0.753	0.816
Reader 5	0.713	0.806
Mean	0.702 (0.601, 0.803)	0.823 (0.725, 0.921)

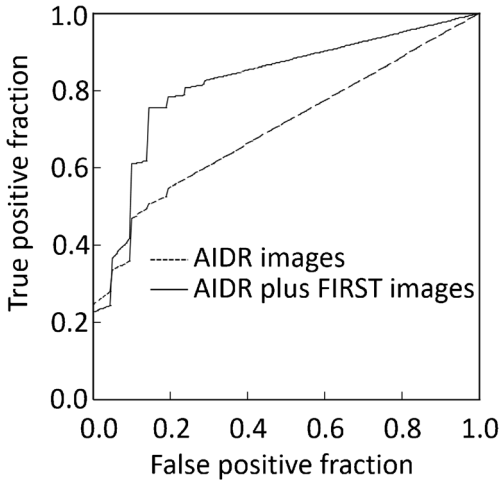

Fig. 4 ROC curves for the detection of neointimal formations after carotid artery stenting. The AUC value was significantly higher on AIDR 3D plus FIRST than AIDR 3D only images (0.82 vs 0.70; $p < 0.01$)

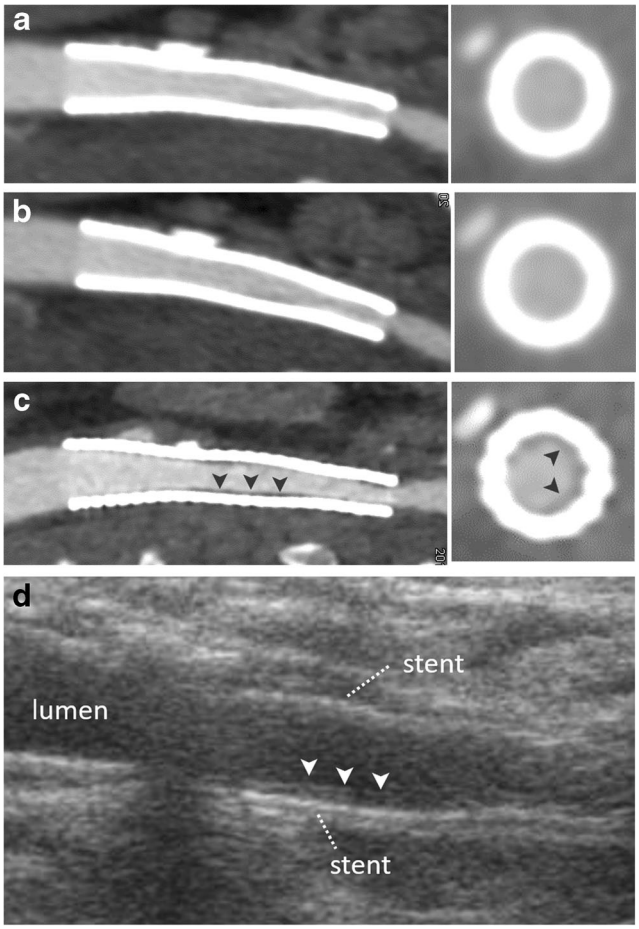

Fig. 5 A 73-year-old man suspected of in-stent restenosis. Curved multiplanar reformation shows a stent in the carotid artery. **a** FBP image. **b** AIDR 3D image. **c** FIRST image. **d** Ultrasound image. The presence of a neointimal formation is difficult to ascertain on FBP (**a**) and AIDR 3D (**b**) images; it is clearly detected on the FIRST image (**c**, *arrowhead*) and confirmed by ultrasonography (**d**, *arrowhead*). *FBP* filtered back projection, *AIDR 3D* three-dimensional adaptive iterative dose reconstruction, *FIRST* forward projected model-based iterative reconstruction solution

Table 5 Kappa coefficients between observers in reading AIDR 3D and AIDR 3D plus FIRST images

	Observer 1	Observer 2	Observer 3	Observer 4
Reading of the AIDR 3D images				
Observer 2	0.72			
Observer 3	0.84	0.56		
Observer 4	0.86	0.75	0.91	
Observer 5	0.50	0.75	0.51	0.44
Reading of the AIDR 3D plus FIRST images				
Observer 2	0.76			
Observer 3	0.64	0.56		
Observer 4	0.83	0.73	0.62	
Observer 5	0.70	0.66	0.61	0.71

resolution is higher than on images reconstructed with conventional FBP or hybrid IR [10, 11]. Tatsugami et al [12] who examined the effect of model-based IR on the image quality of coronary artery stents found that the stent strut was sharper and the attenuation effects from stent struts were lower on model-based than hybrid IR images.

In this study, we firstly compared the usefulness of FBP and two IR methods for the detection of simulated neointimal formations in a CAS phantom. On FIRST, but not on FBP and AIDR 3D images, neointimal formations such as 0.4 mm or 0.6 mm were visualised. In addition, the difference between the measured and the true diameter of the simulated neointimal formations was smaller on FIRST than FBP or AIDR 3D images. As the stent material is thought to be a major factor with respect to diagnostic accuracy and lumen visibility, we evaluated the WALLSTENT and the PRECISE stent in the phantom study. On FIRST images, the recorded diameter of the simulated neointimal formations was not affected by the stent material.

In the clinical study, measured values of neointimal formations were more accurate on FIRST than AIDR 3D images. Also, the diagnostic performance for the detection of neointimal formations was better on FIRST images. The higher sensitivity on FIRST than AIDR 3D images (84% vs 58%) suggests that neointimal formations are not likely to be missed on FIRST images. Consequently, in-stent neointimal formations that may have been overlooked on images acquired with conventional methods may be identified on subsequent studies using FIRST. On the other hand, as the NPV was higher on FIRST than AIDR 3D images (82% vs 67%), we suggest that the FIRST images are useful for the exclusion of neointimal formations. It is uncertain whether clinical management will change dramatically by detecting the neointimal formations from the very early stage. However, for these patients, we can suggest more rigid control of blood pressure or hyperlipidaemia. So, we consider that the use of FIRST may decrease the future risks of restenosis or cerebral infarction.

Our study has some limitations. First, the small number of patients limits the informational value of our findings. Second, we investigated the effect of IR algorithms on a CT scanner from a single vendor; the use of scanners from other vendors may result in different findings. Third, although the readers were blinded to the reconstruction method used (AIDR 3D or FIRST), it may have been obvious due to major differences in the image characteristics.

In conclusion, the model-based IR algorithm improves diagnostic performance for the detection of neointimal formations after CAS.

Funding The authors state that this work has not received any funding.

Compliance with ethical standards

Guarantor The scientific guarantor of this publication is Kazuo Awai.

Conflict of interest Kazuo Awai, Professor of Hiroshima University, obtained a research grant from Canon Medical Systems. The other authors of this manuscript declare no relationships with any companies, whose products or services may be related to the subject matter of the article.

Statistics and biometry One of the authors (F.T.) who has skill for statistics performed the statistical analyses.

Informed consent Written informed consent was obtained from all subjects in this study.

Ethical approval Institutional Review Board approved this study.

Methodology
- retrospective
- diagnostic or prognostic study
- performed at one institution

References

1. North American Symptomatic Carotid Endarterectomy Trial C, HJM B, Taylor DW et al (1991) Beneficial effect of carotid endarterectomy in symptomatic patients with high-grade carotid stenosis. N Engl J Med 325:445–453
2. Walker MD, Marler JR, Goldstein M et al (1995) Endarterectomy for asymptomatic carotid artery stenosis. JAMA 273:1421–1428
3. Yadav JS, Wholey MH, Kuntz RE et al (2004) Protected carotid-artery stenting versus endarterectomy in high-risk patients. N Engl J Med 351:1493–1501
4. Groschel K, Riecker A, Schulz JB, Ernemann U, Kastrup A (2005) Systematic review of early recurrent stenosis after carotid angioplasty and stenting. Stroke 36:367–373
5. Lal BK, Beach KW, Roubin GS et al (2012) Restenosis after carotid artery stenting and endarterectomy: a secondary analysis of CREST, a randomised controlled trial. Lancet Neurol 11:755–763
6. Bonati LH, Dobson J, Featherstone RL et al (2015) Long-term outcomes after stenting versus endarterectomy for treatment of symptomatic carotid stenosis: the International Carotid Stenting Study (ICSS) randomised trial. Lancet 385:529–538
7. Dahl JJ, Dumont DM, Allen JD, Miller EM, Trahey GE (2009) Acoustic radiation force impulse imaging for noninvasive characterization of carotid artery atherosclerotic plaques: a feasibility study. Ultrasound Med Biol 35:707–716
8. Rongling L, Bruce B, Patricia A (1994) B-mode-detected carotid artery plaque in a general population. Stroke 25:2377–2383
9. Geyer LL, Schoepf UJ, Meinel FG et al (2015) State of the art: iterative CT reconstruction techniques. Radiology 276:339–357
10. Nelson RC, Feuerlein S, Boll DT (2011) New iterative reconstruction techniques for cardiovascular computed tomography: how do they work, and what are the advantages and disadvantages? J Cardiovasc Comput Tomogr 5:286–292
11. Fujita M, Higaki T, Awaya Y et al (2017) Lung cancer screening with ultra-low dose CT using full iterative reconstruction. Jpn J Radiol 35:179–189
12. Tatsugami F, Higaki T, Sakane H et al (2017) Coronary artery stent evaluation with model-based iterative reconstruction at coronary CT angiography. Acad Radiol 24:975–981
13. Hillis SL, Berbaum KS, Metz CE (2008) Recent developments in the Dorfman-Berbaum-Metz procedure for multireader ROC study analysis. Acad Radiol 15:647–661
14. Bonati LH, Ederle J, McCabe DJ et al (2009) Long-term risk of carotid restenosis in patients randomly assigned to endovascular treatment or endarterectomy in the Carotid and Vertebral Artery Transluminal Angioplasty Study (CAVATAS): long-term follow-up of a randomised trial. Lancet Neurol 8:908–917
15. Arquizan C, Trinquart L, Touboul P-J et al (2011) Restenosis is more frequent after carotid stenting than after endarterectomy. Stroke 42:1015–1020
16. Silver FL, Mackey A, Clark WM et al (2011) Safety of stenting and endarterectomy by symptomatic status in the Carotid Revascularization Endarterectomy Versus Stenting Trial (CREST). Stroke 42:675–680
17. Hou Y, Xu S, Guo W, Vembar M, Guo Q (2012) The optimal dose reduction level using iterative reconstruction with prospective ECG-triggered coronary CTA using 256-slice MDCT. Eur J Radiol 81:3905–3911
18. Tomizawa N, Nojo T, Akahane M, Torigoe R, Kiryu S, Ohtomo K (2012) Adaptive iterative dose reduction in coronary CT angiography using 320-row CT: assessment of radiation dose reduction and image quality. J Cardiovasc Comput Tomogr 6:318–324